Original Research Article

Modulation mechanism of Proanthocyanidins from Leaves of Bayberry (Myrica rubra Sieb. Et Zucc.) on hyperlipemic rats induced by high-fat-diet

ABSTRACT

Aim: The present study aims to investigate the lipid-lowering effect of Proanthocyanidins from Bayberry leaf (BLP) in rat model of hyperlipemia and to clarify the underlying molecular mechanism.
Study design: The study includes in-vitro assays and in-vivo study in rat model.
Place and Duration of Study: College of Life Sciences, China Jiliang University, Zhejiang Province, China, between March 2021 to December 2021.
Methodology: BLP extracts were preliminarily characterized. The adsorption rate of BLP was determined based on in vitro binding to bile acids. The effect of BLP on membrane transport of bile acids was examined through Caco-2 monolayer in trans-well. The effect of BLP on high-fat-feed rat serum enzyme activity and lipid metabolism genes expression.
Results: Total polyphenol and proanthocyanidins contents were 97.93% and 82.25% using gallic acid and Epigallocatechin-3-O-Gallate (EGCG) as equivalent, respectively. The total flavonoid content was 12.05% (quercetin as equivalent). The average polymerization degree of BLP was determined as 4.51, and in vitro average binding rates of BLP to bile acids were all greater than 80%. BLP significantly obstructed membrane transport of bile acids in Caco-2 monolayer cells. TG, TC and LDL-C concentrations in rat serum were markedly decreased after 28-day BLP treatment. Hepatic steatosis was significantly ameliorated in high-dose GLP treatment group compared with high fat group. High-dose administration of BLP resulted in significantly reduced levels of HMG-CoA reductase, and significantly increased levels of ABCG5, LXR-α receptor and CYP7A1 in rat tissue.
Conclusion: BLP mediates serum lipid metabolism via preventing bile acids re-absorption and regulating the expression of lipid metabolism-related genes.

Keywords: Bayberry leaf proanthocyanidins (BLP); bile acids; hyperlipemia; lipid metabolism regulation

Comment [a1]: Please insert the full name beside abbreviations when mentioned for first time in abstract section

1. INTRODUCTION

Comment [a2]: Please shorten the sentences in introduction section

In recent years, hyperlipemia, atherosclerosis and related coronary heart disease have become increasingly prevalent chronic diseases that threat human health around the globe. Accumulating evidence suggest that excessive production of superoxide in the arterial vessels of high-fat-diet animals [1], and increased oxygen-free radical production to suppress nitric oxide generation are closely related to chronic inflammation [2]. Furthermore, these risk factors, including oxidized low-density lipoprotein (oxLDL), play a critical role in early atherogenesis, endothelial cell injury and macrophage activation. The accumulation of lipid compositions, such as cholesterol and triglyceride, by the macrophage and foam cells to subsequently compose fatty streak is hallmark of early lesion, followed by the development of fibrous and atheromatous plaques [3]. Therefore, maintaining balance in blood lipid levels is of critical importance to prevent the incidence of coronary disease.

Proanthocyanidins belongs to a generic term of flavanols and is widely distributed in plants. ~~Researches~~ Researchers reported that proanthocyanidins exhibit certain promising functions, such as anti-oxidation, free radical scavenging, anti-microbial, anti-cancer and protection against heart cerebrovascular disease [4-5]. Especially, the efficacy of grape seed proanthocyanidins extract (GSPE) has been reported in the treatment of cardiovascular disease [6-7]. Some researchers have developed the mechanism with respect to miRNA modulation, bile acids and cholesterol excretion, as well as the aberrant expression of lipid metabolism-related genes [8-10]. However, the molecular mechanism of modulating lipid metabolism remains to be clarified.

Bayberry leaf proanthocyanidins (BLP) is a main kind of natural product in our lab; the isolation and identification of BLP have been well developed in our previous work [11]. The characterization results showed that BLP has a distinctive cyanidin structure and that its basic structure unit is mostly composed of Epigallocatechin-3-O-Gallate (EGCG), which exhibited obvious difference from GSPE. Researchers in our lab have developed the overall assessment of BLP anti-oxidation [12]. The evaluation results showed that the free-radical scavenging capacity and reducing capacity of BLP is greater than GSPE. Moreover, the lipid antioxidative capacity of BLP was higher than 2, 6-di-tert-butyl-4-methylphenol (BHT). However, the molecular modulation mechanism of BLP on hyperlipemia, except for those in vitro anti-oxidation assessments, remains unclear and therefore requires comprehensive investigations.

In the present study, BLP was isolated and purified from Bayberry leaf and its modulation mechanism on hyperlipemia was evaluated comprehensively using assays of in vitro binding of bile acids, membrane transport of bile acids, rat serum enzyme activity and lipid metabolism genes expression, in an attempt to clarify the regulation mechanism of BLP in lipid metabolism from multiple perspectives.

2. MATERIAL AND METHODS

2.1 Materials

BLP was isolated and purified in our lab. Chemical and biochemical reagents, such as cholalin (SC), glycocholic acid (SGC), taurocholic acid (STC), glycodesoxycholic acid (GCA), turo-ursodesoxycholic acid (TUCA), taurolithocholic acid (TCA), glycochenodeoxycholic acid (GCDA), cholestyramine, furaldehyde and pancreatin (Protease 4080U/g, Lipase 33600U/g and Amylase 91000U/g), were purchased from J&K Chemicals Ltd. (Shanghai, China). All above chemical reagents purity were higher than 98%. Caco-2 cell was purchased from Cell Resource Center of Shanghai Institute of Life Sciences, Chinese Academy of Sciences (CRC, CAS). BCA protein assay kit was purchased from Beyotime Institute of Biotechnology (Jiangsu, China).

2.2 BLP preparation and preliminary characterization

2.2.1 BLP preparation and purification

The preparation procedures were conducted in accordance to reported literature except for minor modification [16]. One-kilogram dried bayberry leaf was used to obtain 150g crude extract by using freeze-drying method. The crude extracts were isolated and purified in D101 macroreticular resin column and the residue was treated by Sephadex LH-20 column, and was in turn eluted by methanol-water (9:1, v/v), acetone-water (1:1, v/v) and acetone-water

(7:3, v/v). Finally, acetone-water (1:1, v/v) elution (named as fraction II) was collected in flask for subsequent assay.

2.2.2 Determination of total polyphenol content (TPC) in BLP

TPC in BLP was determined by using Folin Ciocalteu's colorimetric method described by Gao et al [13]. Total polyphenol content was calculated as gallic acid equivalent (GAE) in mg/mL of reaction mixture on the basis of calibration curve of gallic acid, $Y=2.5486X+0.2785$, $R^2=0.9966$, where X refers to gallic acid concentration and Y indicates absorbance. Lastly, TPC (mg/mg) was calculated as (BLP concentration (mg/mL) × reaction solution volume (mL) × dilution factor) / BLP mass (mg).

2.2.3 Determination of total proanthocyanidin content (TPCC) in BLP

Refer to the method described by Sun et al [14]. Total proanthocyanidin content was calculated as EGCG equivalent (EAE) in mg/mL of reaction mixture, according to the calibration curve of EGCG ($Y=4.843X+0.0992$, $R^2=0.9982$, where X indicates EGCG concentration and Y absorbance). Lastly, TPCC (mg/mg) was estimated as (BLP concentration (mg/mL) × reaction solution volume (mL) × dilution factor) / BLP mass (mg).

2.2.4 Determination of total flavonoid content (TFC) in BLP

Refer to the method described by Ordonez et al [15]. Total flavonoid content was calculated as quercetin equivalent (QAE) in mg/mL of reaction mixture on the basis of calibration curve of quercetin ($Y=8.285X+0.812$, $R^2=0.9959$, where X represents quercetin concentration and Y absorbance). Lastly, TFC (mg/mg) was estimated as (BLP concentration (mg/mL) × reaction solution volume (mL) × dilution factor) / BLP mass (mg).

2.2.5 Estimation of average degree of polymerization (ADP) of BLP

Refer to the method elaborated by Blutler et al [16]. Total proanthocyanidin molar concentration was calculated according to the calibration curve of EGCG: $Y=2.2031X+0.1087$, $R^2=0.9983$, where X was EGCG molar concentration (mmol/L) and Y was the absorbance. Total proanthocyanidin molar (mmol) was estimated as BLP concentration (mmol/L) × reaction volume (L) × dilution factor. Therefore, ADP was calculated by the formula, ADP=m/(M×n), where m was BLP mass (mg), n was BLP amount of substance (mmol) and M was relative molecular weight of EGCG.

2.3 In vitro assays

2.3.1 In vitro binding capacity of BLP to bile acids

The in vitro bile acids (C, TA and GA) binding procedure was conducted according to the method described by Kahlon et al (2007) and Deng et al (2011) [17-18], with minor modification. After 10 mg BLP (fraction II) was digested in 1 mL 0.01M HCL solution for one hour at 37^{o}C in the shaker, the pH value of the sample was adjusted to 6.3 by adding 0.1 mL 0.1 M NaOH. Each test sample was added with 4 mL of bile acid mixture working solution (0.3 mmol/L SC, STC or SGC) in a 0.1 M phosphate buffer (pH 6.3). Then 4 mL phosphate buffer was added into the individual substrate blanks. After 5 mL of porcine pancreatin (10 mg/mL, in a 0.1 M phosphate buffer, pH 6.3) was added, the tubes were incubated for 1h at 37^{o}C in a shaker. The mixtures were centrifuged in an ultracentrifuge (18000 r/min) for 20 min at 25^{o}C. Then the supernatant was collected and the absorbance of bile acid was

detected at 387 nm. Bile acid concentration was calculated according to the calibration curve of the responding bile acids.

SC: Y=0.0104X-0.0589, R^2=0.9978;
STA: Y=0.0104X-0.0589, R^2=0.9978;
SGA: Y=0.0104X-0.0589, R^2=0.9978;

Where X was bile acid concentration, Y was absorbance. The relative in vitro bile acid binding was calculated as (total concentration – supernatant concentration) / total concentration.

The procedures were conducted in accordance with the progress mentioned above, except for the bile acid mixture working solution (0.3 mmol/L C, TA or GA) was replaced with other solution (0.3 mmol/L GCA, TCA, TUCA or GCDA). 1 mL supernatant was added with 1 mL acetic acid solution (60%, v/v) and 2 ml furaldehyde solution (1%, v/v)in a tube. After vortex-mix, the tube was incubated in ice-bath for 2 min, and was then added with 6 mL H_2SO_4 solution (50 mL H_2SO_4: 65 mL H_2O, v/v) and incubated at 70^oC for 10 min after vortex-mix. After that, the tube was incubated in ice-bath for 5 mins and the absorbance of bile acid was detected at 650 nm. The responding calibration curve of individual bile acid was as follows:

GCA: Y=0.0104X-0.0589, R^2=0.9978;
TCA: Y=0.0104X-0.0589, R^2=0.9978;
TUCA: Y=0.0104X-0.0589, R^2=0.9978;
GCDA: Y=0.0104X-0.0589, R^2=0.9978.

Considering cholestyramine as 100 bound, the relative in vitro bile acid bindings was calculated as (total concentration – supernatant concentration) / total concentration.

2.3.2 Effect of BLP on membrane transport of bile acids in Caco-2 monolayer cell model

Three experiment groups, including blank culture medium group, bile acids group and BLP + bile acids group, were established in Caco-2 monolayer model. Caco-2 cells were cultured in trans-well (Corning products, USA) in the 6-well cell culture plate with DMEM culture medium at 37^oC (containing 5% CO_2 humidified air). When trans-wells were full of Caco-2 cells by observation of inverted microscope, cell monolayer permeability and polarization were assessed by phenolsulfonphthalein permeation content and alkaline phosphatase activity, respectively.

Afterwards, the apical side (AP) of Caco-2 monolayer in trans-well was washed with 2.5 mmol/L bile acid solution (TA and GA) or 1 mg/mL BLP + 2.5 mmol/L bile acid solutions (1.5mL) by HBSS (Hank's Balanced Salt Solution). HBSS (2.5mL) was poured onto the Basolateral side (BL) of Caco-2 monolayer, and then 0.1 mL HBSS solution was taken out from the basolateral side, and the same volume of blank HBSS solution was simultaneously supplemented at 0, 2, 4, 8h. The bile acid (TA and GA) concentrations in HBSS buffer solution from basolateral side were measured by using RP-HPLC [19]. Bile acid quantity was calculated according to the volume of the culture medium, so as to analyze the effect of BLP on membrane transport of bile acid.

2.4 In vivo assays

2.4.1 Animals and experimental setup

Comment [a3]: Please insert period of acclimatization, environment in which rats were reared and diet and water administered?

Twenty-four male Wistar rats (221.7±10.3g) were randomly divided into four groups: (A) normal control group (n=6), rats received oral administration of normal saline at 5 ml/kg body weight (BW) once per day; (B) high fat diet group (n=6), rats received oral administration of normal saline at 5 ml/kg body weight per rat once per day with simultaneous high-fat-diet feed; (C) low-dose BLP group (n=6), rats received oral administration of BLP components at a dose of 100 mg/kg (5 ml/kg body weight per rat once per day) with simultaneous high-fat-diet feed; (D) high-dose BLP group (n=6), rats received oral administration of BLP components at a dose of 200 mg/kg (5 ml/kg body weight per rat once per day) with simultaneous high-fat-diet feed. Same treatment continued for 28 days. The high-fat-feed, which contains 79% basal feed, 1% cholesterol, 10% lard, and 10% yolk powder, was purchased from Jiangsu XieTong Organism Ltd. (Nanjing, Jiangsu, China).

Comment [a4]: Add age of rats please.

Comment [a5]: Why authors selected these doses? ? Please insert reference if present

2.4.2 Body and liver weights

Experimental rats were weighed once every week. 24h after the final oral administration, the body weights of the rats were measured and their blood was collected from the inferior vena cava. Livers and small intestines were separated, and the weights of rat livers were determined. Serum was stored at -80 ^{o}C after separation prior to following experiments. Part of liver and small intestine was frozen in liquid nitrogen.

Comment [a6]: Please rewrite and determine tissue samples taken for histopathological examining, PCR, and western blotting

2.4.3 Serum biochemical analysis

Serum alanine aminotransferase (ALT) and aspartate aminotransferase (AST) activities were determined by using commercial kits (Nanjing Jiancheng Bioengineering Institute (Nanjing, China). The levels of total cholesterol (TC), triglyceride (TG), low density lipoprotein cholesterol (LDL-C), high density lipoprotein cholesterol (HDL-C), adiponectin (ADPN), leptin (LEP), malonaldehyde (MDA), glutathione (GSH), alkaline phosphatase (ALP) and total bile acids (TBA) in rat serum were analyzed by using commercialized kits (Biosino Biotechnology Co., Ltd., Beijing, China), following the manufacturer's instruction. Moreover, TBA content in rat feces was also tested according to established method.

2.4.4 Concentration of bile acids in rat serum

Bile acids concentration was determined according to previous methods with a brief modification [20]. A rat serum sample (0.1 mL) was and 0.3 mL methanol was vortex-mixed for 1 min. After centrifugation (18000 rpm) for 5 min at 4^{o}C, all the supernatant was evaporated to dryness at 40oC under a stream of nitrogen gas. The residue was reconstituted with 0.1 mL initial mobile phase (methanol: 5 mmol/L ammonium acetate with 1% formic acid preparation = 55:45, v/v), vortex-mixed for 1 min and centrifuged (18000 rpm) for 5 min, and then 2μL was injected into the LC-qTOF-MS system.

The WATERS UPLC system (Waters Corp., Singapore) is composed of a quaternary gradient pump and a UV detector. ACQUITY UPLC BEH C18 column (1.7 μm, 50 × 1.0 mm) was used for analysis. The flow rate was 0.3 ml/min, the temperature of the column was kept at 45 ^{o}C, and the UV detector wavelength was set at 254 nm. The AB Triple TOF 5600 plus System (AB SCIEX, Singapore) was used for quantitative mass spectrometric detection. The mass spectrometer was operated in the negative mode to generate (M-H)-ions. The capillary voltage was 3.5 KV and the cone voltage was 50V. The ionization resource worked at 120^{o}C, and the desolvation temperature was set at 270^{o}C. Nitrogen, at a flow rate of 300 L/h and 60 L/h, was used as desolvation and cone gas, respectively. Instrument control, data acquisition and analysis were performed by using the MasslynxTM 6.0 data system software.

2.4.5 Histological staining of liver

Liver samples from all rats were processed for light microscopy. Liver slices were obtained from the distal portion of the left lateral lobe and the tissue was fixed for at least 48 h in 10% neutral-buffered formalin. The samples were then embedded in paraffin, cut into 5-μm sections, and stained with haematoxylin and eosin (H&E) for examination by light microscopy.

2.4.6 Reverse transcription and quantitative real-time PCR detection

Total RNA was extracted using TRI-Reagent® (Haogene Biotech, Hangzhou, China) and was quantitated by using spectrophotometric analysis. Reverse transcription was performed using SuperScript II Reverse Transcriptase™ and RNasin (Invitrogen, USA) according to the manufacturer's protocol. Quantitative real-time polymerase chain reaction (qRT-PCR) was performed using the Brilliant SYBR Green Master Mix (Bio-Rad Laboratories, Hercules, USA). The mRNA levels of liver sterol regulatory element-binding protein-2 (SREBP-2), 3-hydroxy-3-3methylglutary-CoA (HMG-CoA) reductase, liver X receptor-α (LXR-α), cholesterol-7α-hydroxylase (CYP7A1) and intestinal Niemann-Pick C1 like 1 (small intestine NPC1L1), ATP binding cassette transporters (ABCG-5), cholesterol acyltransferase (ACAT-2) and microsomal triglyceride protein (MTP) were evaluated in qRT-PCR assay. The primers used for PCR amplification are listed in Tab 1. Rat 18S rRNA was used as an internal reference gene according to previous study [21]. All oligonucleotide primers were synthesised by Shanghai Sangon Biotech (Shanghai, China). All values were calculated using the delta delta Ct method and were expressed as fold-change relative to 18S rRNA.

Comment [a7]: Please determine tissue used for real time PCR.

Table 1. Primer Sequences for Quantitative Real-time Polymerase Reaction

Comment [a8]: Please add references for used primers.

Gene name	Forward	Reverse
Rat SREBP-2	CTGGAGGCTGGTTTGACTGGAT	GTGACCGAGGAGCGTGAGTGT
Rat HMG-CoA	CCTGCGTGTCCCTGGTCCTA	CCTTTGGGTTACTGGGTTTGGT
Rat LXR-α	CTGATGTTCCCACGGATGCTAAT	CCAACACAGAGGACACGGAGAA
Rat CYP7A1	CAAGACGCACCTCGCTATTCTCT	CTTCAGAGGCTGCTTTCATTGCT
Rat NPC1L1	GCTGCTGTTTCTGACCCTGTTT	CCCACTTCAAGGTATCGGTTCAG
Rat ABCG-5	CTTCTGTGCCAAATAACCCAATG	GGATGACAAGAGTCGGGATGAA
Rat ACAT-2	GACTTCATTGATGAGGGCAGGTT	GAAGCAGCGTGGACAGGAACAT
Rat MTP	GTTCTCCCAGTACCCGTTCTTGGT	CCTCCCTGTGGATAGCCTTTCAT
Rat 18s	GAATTCCCAGTAAGTGCGGGTCATA	CGAGGGCCTCACTAAACCATC

2.4.7 Western blotting

Western blotting assay was conducted to quantitatively investigate the effect of BLP treatment on protein expression of CYP7A1, LXR-α, HMG-CoA reductase in liver tissue and

ABCG-5 in small intestine tissue. Liver and small intestine tissues were washed with cold PBS and lysed by using lysis buffer containing protease inhibitor cocktail. Protein concentrations were determined using commercialized BCA detection kit (Beyotime Products, Shanghai, China). Then, tissue extracts (50 μg per sample) were separated via 10% gel electrophoresis and electro-blotted onto the PVDF membrane (Merck Millipore). Non-specific binding sites were blocked by incubating the PVDF membrane for 1h in PBS containing 5% non-fat dry milk. Membranes were probed with primary antibodies overnight at 4°C, followed by incubation of horseradish peroxidase (HRP)-conjugated second antibody. Blots were developed using an enhanced chemiluminescence detection system (ECL; Amersham Pharmacia Biotech, Piscataway, NJ, USA) according to the manufacturer's instructions. β-actin was used as the internal reference protein.

2.5 Statistics

Data were expressed in the form of means ± standard deviation (SD). Statistical comparison between groups was performed using ANOVA or nonparametric Mann-Whitney U test (two-tailed) followed by Bonferroni's multiple comparisons test for group comparisons in the SPSS (version 18.0). A probability of $P < .05$ was considered to indicate statistical significance.

3. RESULTS

3.1 ~~hytochemical~~ Phytochemical compositions and ADP of BLP

TPC, TPCC and TFC of extracts were expressed in the form of mg GAE/ mg BLP, mg EAE/ mg BLP and mg QAE/mg BLP, respectively. In our current study, TPC, TPCC and TFC (%) were 97.93%±1.46%, 82.25%±1.53% and 12.05%±0.52%, respectively. All the content results were expressed based on three replicates. The ADP result of BLP was nearly 4.51.

3.2 In vitro BLP binding to bile acids

The binding capacity of individual bile acid was determined in this study, and the results were listed in Fig 1. Apparently, the average binding rates of BLP to all types of bile acids were higher than 80% and the highest binding rate was GCA. The binding rates of BLP to SGC, STC and GCDA were relatively lower than the other bile acids in this experiment (Fig 1).

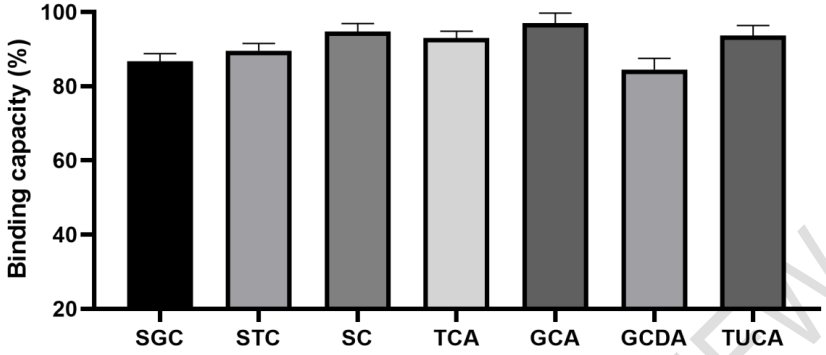

Fig. 1. The binding capacity of BLP to bile acids

3.3 Inhibition of BLP on membrane transport of bile acids in Caco-2 monolayer

Quantities of bile acid was detected by the HPLC system (SHIMADZU-20AT series equipment) with a UV detector and a Zhida N2000 instrument workstation in Zhejiang University. EGCG separation was achieved by using a Hypersil BDS C18 reversed-phase column (5 μm, 250 mm×4.6 mm). The mobile phase was composed of methanol and 0.6% KH2PO4 solution (65:35, V/V) at a flow-rate of 1.0 mL/min. The column temperature was kept at 40^{o}C and the detector wavelength was set at 205 nm. The concentrations of bile acids were calculated on the basis of calibration curve of bile acids. SGC: Y=631568X-2740.8, R^2=0.9998; STC: Y=381123X-758.8, R^2=0.9998; where X was bile acid concentration and Y was peak area. Bile acid quantity (μmol) was calculated as bile acid concentration (μmol/mL) × culture medium volume in BL side (mL). The inhibition results (Fig 2.) show that bile acid quantities with BLP at 4h and 8h were significantly down-regulated than those without BLP. These data suggested that BLP exhibits pronounced inhibitive effect upon the membrane transport of bile acids.

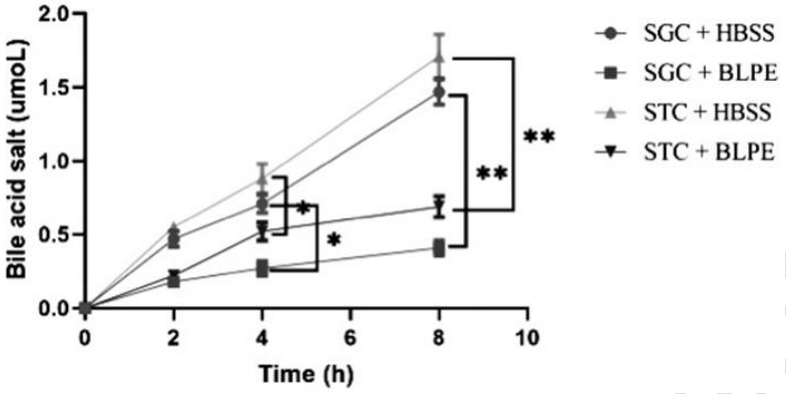

Fig. 2. BLP exhibits markedly suppressive effect on membrane transport of SGC and STC

*Values are expressed as means ± SD (n=6). * P<0.05, ** P<0.01.*

3.4 Body and liver weights

Statistically increased mean body weight was observed in the model group in the third week and the fourth week, compared with the normal group. The mean weights in high-dose BLP were significantly decreased compared with those of the model group in the third and the fourth week, and no significant differences were observed between low-dose and high-dose BLP groups. However, no significant differences in liver weight were determined among the four groups. Liver index was increased significantly in the model group as compared with the normal group. Further, no marked difference in the liver index could be found between low-dose group and high-dose group, and the liver index of the two groups were not significantly different from that of the model group. All the above results are listed in Table 2.

Table 2. Mean body and liver weights and liver index ($\bar{x}$±s, gram, n=6)

Groups	Body weight (3rd Week)	Body weight (4th Week)	Liver weight	Liver Index (%)
Normal control	354.50±9.93	374.33±18.97	19.85±2.14	0.053±0.0065
High-fat-diet	376.00±10.37[a]	405.50±13.03[a]	22.70±1.66[a]	0.056±0.0041
Low-dose	355.33±24.86	379.67±28.35	21.17±2.41	0.056±0.0045
High-dose	340.67±14.76[b]	352.83±12.28[b]	20.07±0.95	0.060±0.0033

[a]P < .05 as compared with normal group; [b]P < .05 as compared with model group.

3.5 Effect of BLP on biochemical parameters in serum

All the biochemical parameters in rat serum were calculated by using commercialized kits and the results were listed in Tab 3 and Tab 4. Compared with model group, the contents of TC, TG, and LDL-C were significantly decreased in high-dose BLP group. The content of HDL-C and LEP was markedly increased in high-dose of BLP group, while the serum contents of ADPN exhibited no significant difference. Besides, the concentrations of AST, ALT and MDA were significantly lower in high-dose group than in model group. Compared with model group, the concentration of GSH was significantly increased in both two BLP treatment groups. However, the concentrations of ASP and TBA in rat serum exhibited no significant difference between model group and BLP treatment groups. Moreover, TBA content in rat feces was also calculated, and the contents in the four groups were 20.27±5.71, 31.65±4.44, 43.09±9.65 and 55.66±9.12 mg/g dried feces, respectively. Compared with normal group and model group, the fecal TBA content in high-dose BLP group was significantly higher.

Table 3. Levels of TG, TC, LDL-C, HDL-C, LEP and ADPN in rat serum ($\bar{x}$±s, mmol/L, n=6)

Experimental groups	TC	TG	LDL-C	HDL-C	LEP	ADPN
Normal control	3.51±0.69	3.57±0.38	0.67±0.23	1.69±0.49	2.96±0.41	2.78±0.82
High-fat-diet	6.65±1.61 [a]	8.63±1.14 [a]	1.44±0.27 [a]	0.99±0.32 [a]	2.27±0.31 [a]	2.18±0.60
Low-dose	7.63±1.71	7.18±1.58	0.81±0.55 [b]	1.18±0.48	2.82±0.71 [b]	2.84±0.91
High-dose	5.36±0.67 [b]	5.48±1.38 [b]	0.83±0.60 [b]	1.27±0.37 [b]	2.89±0.52 [b]	2.77±0.76

[a]P < .05 as compared with normal group. [b]P < .05 as compared with model group.

Comment [a9]: Insert units of measuring and please insert abbreviations in the footnotes and the same for all other tables.

Table 4. Levels of AST, ALT, MDA, GSH, ALP and TBA in rat serum ($\bar{x}$±s, mmol/L, n=6) .

Groups	AST	ALT	MDA	GSH	ALP	TBA
Normal control	378.43±109.34	186.83±29.57	3.98±0.46	83.64±19.73	4.17±1.92	354.13±135.17
High-fat-diet	548.52±138.9[a]	564.87±60.02[a]	6.46±1.27[a]	52.54±15.17[a]	7.39±3.49[a]	882.85±245.95[a]
Low-	428.70±113.	320.22±106	3.98±0.41[b]	246.55±134	6.66±3.62	809.88±219.

dose	52	.87		.87[b]		10[a]
High-dose	349.86±98.69[b]	168.23±58.15[b]	3.75±0.23[b]	251.42±115.37[b]	8.23±2.56[a]	740.25±265.19[a]

[a]P < .05 as compared with normal group; [b]P < .05 as compared with model group.

3.6 Concentrations of bile acids in rat serum

The results of contents of bile acids in rat serum found markedly differences between different groups. Several bile acids were not detected in model group and high-dose BLP treatment group, including SC, TCA, GCA and TUCA. STC concentration in model control group was significantly higher than in normal control group, whereas no significant difference in glycocholic acid (SGC) concentration was observed between normal control group and high-dose group. SGC concentration was markedly increased in model control group, while no different GCDA concentration was determined among three groups. All the detected results were listed in Table 5.

Table 5. Contents of serum bile acids were measured by UPLC-qTOF-MS ($\bar{x}$±s, ng/mL, n=6)

BA	Normal control	Model control	High-dose BLP group
TCA	89.88±36.96	ND	ND
STC	42.88±25.89	69.77±15.78 [a]	ND
SGC	421.31±125.13	640.29±119.01	492.35±78.85 [b]
GCDA	1435.32±314.80	1409.29±261.84 [a]	1562.44±483.83 [a]
SC	217.56±66.02	ND	ND
GCA	358.41±66.69	ND	ND
TUCA	62.56±12.99	ND	ND

ND: Not Detected; [a]P < .05 as compared with normal group; [b]P < .05 as compared with model group.

3.7 Effect of BLP on liver damage at the histological level

The alleviating effect of BLP treatment on liver damage was evaluated by conducting H&E staining. All these liver tissue sections showed that the central vein was surrounded by hepatic cord cells. The normal control group showed a normal architecture, whereas the model group showed indication of hepatic steatosis (Figs. 3A and 3B). Compared with the normal group, the model group showed steatosis liver tissue architecture. Specifically, an enlarged intercellular space, a wide and big fat vacuole and light cytoplasm staining were observed in the model group. The serious steatosis in liver section was attenuated in low-

dose and high-dose BLP treatment groups (Figs. 3C and 3D), as the BLP treatment group showed less fat vacuole and narrowed intercellular space. Therefore, HE staining results show that steatosis liver morphology was markedly ameliorated by administration of BLP in a dose-dependent manner.

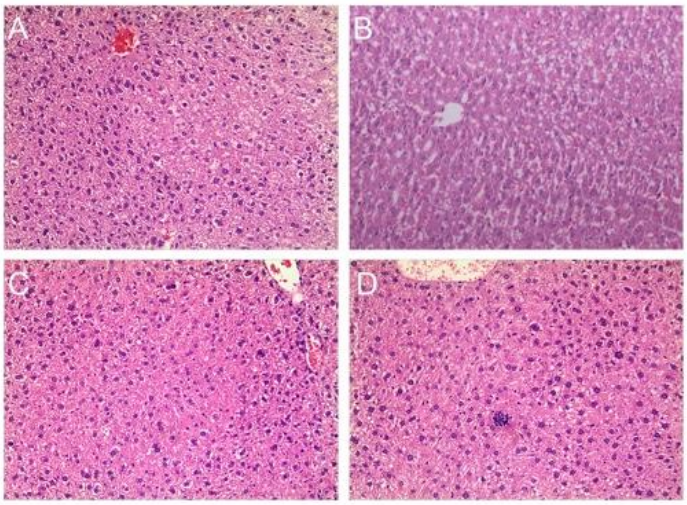

Fig. 3. Liver H&E staining (magnification 200×)
A. Normal control group; H&E staining revealed normal tissue structure, and a regular hepatocyte cord.
B. Model group with high-fat-diet; (an enlarged intercellular space, a wide and big fat vacuole and light cytoplasm staining were observed).
C. Low-dose BLP treatment group;
D. High-dose BLP treatment group; (less fat vacuole, little intercellular space and nearly normal cytoplasm staining were observed).

3.8 Effect of BLP on mRNA levels in rat liver and small intestine

The effects of BLP on the expression of lipid metabolism-related genes, including SREBP-2, HMG-CoA reductase, LXR-α, CYP7A1 in liver tissue and NPC1L1, ABCG-5, ACAT-2 and MTP in small intestine, were analyzed using qRT-PCR assay. The results show that hepatic mRNA HMG-CoA reductase was significantly down-regulated in high-dose BLP group, compared with those in normal control group and model group (Fig. 4). However, liver CYP7A1 and LXR-α receptor level were significantly up-regulated in HBTG group, as opposed to normal control group and high-fat diet model group (Fig. 4). Moreover, ABCG-5 level in small intestine was significantly decreased in model group compared with normal control group, but was significantly increased after oral administration of BLP (Fig. 4). No significantly aberrant levels of SERBP-2, NPC1L1, ACAT-2 and MTP were observed among these groups.

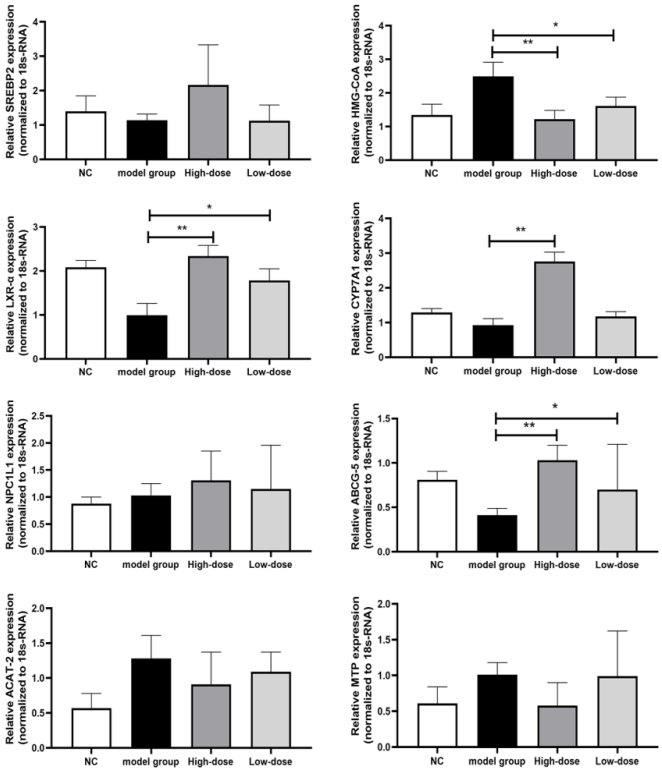

Fig. 4. Effect of BLP on mRNA levels of SREBP-2, HMG-CoA reductase, LXR-α, CYP7A1 and NPC1L1, ABCG-5, ACAT-2 and MTP in rats subjecting to different treatments was analysed.

*Values are expressed as means ± SD (n=6). * P<0.05, ** P<0.01.*

Comment [a10]: Please insert numbers for figures in figure 4 and 5 and clarify which numbers represents in figure legends. And the same for figure 5.

3.9 Analysis of protein expression level by Western blotting

Consistent with the mRNA levels results clarified above, the protein levels of liver CYP7A1, LXR-α, HMG-CoA reductase and intestinal ABCG-5 were determined by western blotting. As illustrated in Fig 5., high-fat-diet feed significantly increased liver HMG-CoA reductase expression compared with that of normal control group. However, liver CYP7A1 receptor expression was markedly up-regulated in both high-dose group and low-dose group, and liver LXR-α expression was significantly augmented in high-dose group. Besides, small intestine ABCG-5 expression was significantly increased in high-dose group than that in the model group.

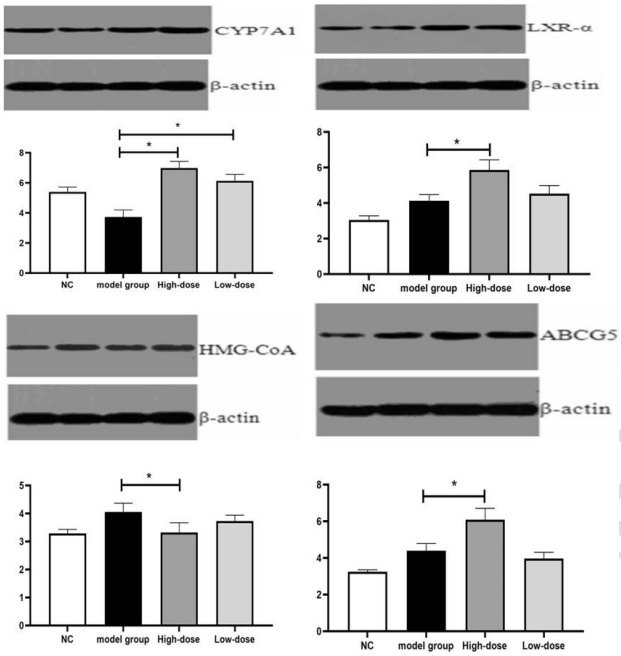

Fig. 5. Effect of BLP on the protein expression of HMG-CoA reductase, LXR-α, CYP7A1 and ABCG-5 in rat.
*Values are expressed as means ± SD (n=6). * P<0.05, ** P<0.01.*

4. RESULTS AND DISCUSSION

Characterization results of BLP showed that the total polyphenol and proanthocyanidins content were 97.93% and 82.25% by using gallic acid and green tea polyphenol EGCG as equivalent, respectively. Suffice it to say that the purified proanthocyanidins from Bayberry leaf is mostly composed of polyphenol ingredients. Lower APD of BLP than the results of Yang et al [11] could be attributed to different methods of characterization.

Herein, we analyzed the binding capacity of EGCG to bile acids, and found that a number of binding rates were greater than some published previous literatures [22-23]. Such disparity could be justified by the fact that BLP is soluble and composed of some EGCG units. EGCG contains eight hydroxyls (OH group), which are more than the other catechins extracted from green tea. Therefore, it is easier for BLP to permeate into the intestinal contents in rats and thereby adsorbing more bile acids through hydrogen bonding. Furthermore, the inhibition of membrane transport of bile acids by BLP was developed in Caco-2 monolayer trans-well plate [24]. Both passive transport and active transport of bile acids through cell membrane can be inhibited by BLP treatment in Caco-2 cells, owing to the hydrogen bonding of BLPE to bile acids. The chemistry mechanism of inhibition transport could be attributed to the various stereo-selectivity of bile acids by BLP, which results to in lower permeability or lower binding capacity with the influx transporters in the cell membrane.

Moreover, we make effort to identify the modulation effect of BLP on hyperlipemic rats induced by high-fat-feed. The results showed that BLP functions to significantly down-regulate blood lipid level in rats. Bile acids levels were markedly regulated in model group and BLP treatment group, compared with the normal control group. Moreover, the aberrant expression of HMG-CoA reductase, CYP7A1 and LXR-α receptor in rat liver were also observed. ABCG-5 expression was significantly decreased in model group compared with normal group, while the expression was significantly increased in BLP-treated group compared with model group. All the changes have comprehensively affected the blood lipid metabolism in rat. Recent researches have analyzed the effect of grape seed proanthacyanidin (GSP) and blueberry leaf polyphenols on modulating lipid metabolism and inhibiting the accumulation of body fat [25, 26]. In weaned pig, GSP affects lipid metabolism via changing gut microflora and enhancing the propionate acid production in pig feces. Thusly, the regulation of BLP on hyperlipemia would be attributed to the change of rat gut microflora.

Moreover, some literatures have reported that the change of bile acids would affect the composition of intestinal flora [27,28], which were relative with the lipid metabolism. Thusly, the effect of BLP on the intestinal flora should be deeply investigated in future studies, along with the clarification of the interaction of BLP, bile acids and intestinal flora (Shown in Fig 6).

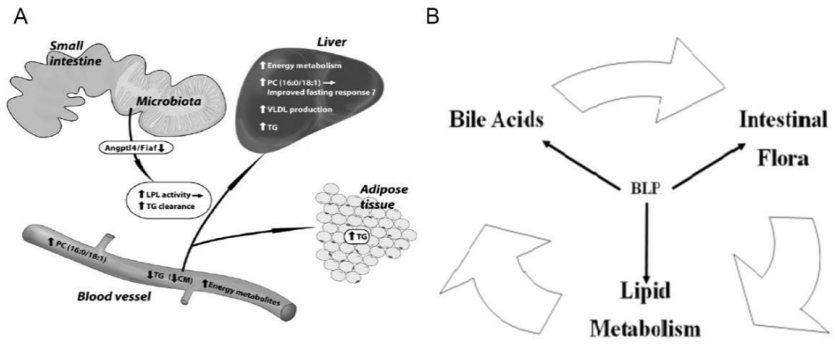

Fig. 6. Interaction and structure of BLP on bile acids and intestinal flora.
(A) Lipid metabolism and intestinal flora and
(B) Interaction diagram of BLP, bile acids and intestinal flora.

5. CONCLUSION

The results obtained in this study indicate that BLP mediates serum lipid metabolism via preventing bile acids re-absorption and regulating the expression of lipid metabolism-related genes. This finding will contribute to the application and development of BLP in the treatment of hyperlipidemia.

CONSENT

It is not applicable

ETHICAL APPROVAL

All the experiments conducted on the animals were in accordance with the standards set for the use of the laboratory animal use and the experimental protocol was approved by the Animal Care Committee of the Zhejiang Laboratory Animal Centre.

COMPETING INTERESTS DISCLAIMER:

Authors have declared that no competing interests exist. The products used for this research are commonly and predominantly use products in our area of research and country. There is absolutely no conflict of interest between the authors and producers of the products because we do not intend to use these products as an avenue for any litigation but for the advancement of knowledge. Also, the research was not funded by the producing company rather it was funded by personal efforts of the authors.

REFERENCES

1. Naplli C, Lerman LO. Involvement of oxidation-sensitive mechanisms in the cardiovascular effects of hypercholesterolemia. Mayo Clin Proc. 2001; 76: 619-631.
2. Kojda G, Harrison D. Interactions between NO and reactive oxygen species: pathophysiological importance in atherosclerosis, hypertension, diabetes and heart failure. Car vas Res. 1999; 43: 562-571.
3. Stocker R, Keaney JF. Role of oxidative modifications in atherosclerosis. Physiol Rev. 2004; 84: 1381-1478.
4. Yamakoshi J, Kataoka S, Koga T, Ariga T. Proanthocyanidin-rich extract from grape seeds attenuates the development of aortic atherosclerosis in cholesterol-fed rabbits. Atherosclerosis. 1999; 142(1): 139-149.
5. Zhang CG, Dong JB, Xie WR. Research progress on antioxidative bioactivities of proanthocyanidins. Cereals & Oils. 2009; 6: 10-12. Chinese.
6. Liu XJ, Qiu J, Zhao SH, et al. Grape proanthocyanidin extract alleviates ouabain-induced vascular remodeling through regulation of endothelial function. Molecular Medicine Reports. 2012; 6 : 949-954. Chinese.
7. Thiruchenduran M, Vijayan NA, Sawaminathan JK, et al. Protective effect of grape seed proanthocyanidins against cholesterol cholic acid diet-induced hypercholesterolemia in rats. Cardiovascular Pathology . 2011; 20: 61-368.
8. Yonguc GN, Dodurga Y, Adigusel E, et al. Grape seed extract has superior beneficial effects than vitamin E on oxidative stress and apoptosis in the hippocampus of streptozotocin induced diabetic rats. Gene. 2015; 555(2): 119-126.
9. Yogalakshmi B, Sreeja S, Geetha R, et al. Grape Seed Proanthocyanidin Rescues Rats from Steatosis: A Comparative and Combination Study with Metformin. Journal of Lipids. 2013; 2013: 153897.
10. Downing LE, Heidker RM, Caiozzi GC, Wong BS, Rodriguez K, Del Rey F, et al. A grape seed procyanidin extract ameliorates fructose-induced hypertriglyceridemia in rats via enhanced fecal bile acid and cholesterol excretion and inhibition of hepatic lipogenesis. PLOS ONE. 2015; 10(10): e0140267.
11. Yang HH, Ye XQ, Liu DH, Chen JC, Shen Y, Yu D. Characterization of unusual proanthocyanidins in Leaves of Bayberry (Myrica rubra Sieb. Et Zucc.). Journal of Agricultural and Food Chemistry. 2011; 59: 1622-1629.
12. YANG HH, YE XQ, SUN YJ, et al. Optimization of extraction of prodelphinidins from bayberry (Myrica rubra Sieb. et Zucc.) leaves. J Food Sci Technol. 2014; 51(10): 2435-2444.
13. Gao X, Bjork L, Trajkovski V, Ugglla M. Evaluation of antioxidant activities of rosehip

ethanol extracts in different test systems. Journal of the Science of Food & Agriculture. 2000; 80(14): 2021-2027.
14. Sun JS, Tsuang YW, Chen I.J, Huang WC, Hang YS, Lu FJ. An ultra-weak chemiluminescence study on oxidative stress in rabbits following acute thermal injury. Burns. 1998; 24(3): 225-231.
15. Ordonez AAL, Gomez JD, Vattuone MA, Isla MI. Antioxidant activities of sechium edule (Jacq.)Swart extracts. Food Chemistry. 2006; 97(3): 452-458.
16. Blutler L G, Price M L, Brotherton J E. Vanillin assay for proanthocyanidins (condensed tannins): Modification of the solvent for estimation of the degree of polymerization. J.Agric.food chem. 1982; 30(6): 1087-1089.
17. Deng ZH, Huang HH. Bile salt-binding capacity and lipid-lowering mechanisms of water extracts from fresh tea leaves and tea flowers. Food Sciences. 2011; 32(19) : 96-99. Chinese.
18. Kahlon TS., Smith GE. In vitro binding of bile acids by blueberries (Vaccinium spp.), plums (Prunus spp.), prunes (Prunus spp.), strawberries (Fragaria Xananassa), cherries (Malpighia punicifolia), cranberries (Vaccinium macrocarpon) and apples (Malus sylvestris). Food chemistry. 2007; 100: 1182-1187.
19. Sakaura H, Suauki M, Kimura N, et al. Simultaneous determination of bile acids in rat bile and serum by HPLC. J Chromatogr. 1993; 621: 123-131.
20. Xu Y, Chen CC, Yang L, et al. Evaluation of hepatotoxicity caused by Dioscorea bulbifera based on analysis of bile acids. Acta Pharmaceutica Sinica. 2011; 46(1): 39-44. Chinese.
21. Sehmittgen TD, Zskrajsek BA. Effect of experimental treatment on housekeeping gene expression validation by real-time, quantitative RT-PCR. J Biochem Biophys Meth. 2000; 46: 69-81.
22. Kahlon TS, Shao Q. In vitro binding of bile acids by soy bean (Glycine max), black eye bean (Vigna unguiculata), garbanzo (Cicer arietinum) and lima bean (Phaseolus lunatus). Food chemistry. 2004; 86: 435-440.
23. Kahlon TS, Chapman MH, Smith GE. In vitro binding of bile acids by spinach, kale, brussels sprouts, broccoli, mustard greens, green bell pepper, cabbage and collards. Food chemistry. 2007; 100: 1531-1536.
24. Sun H, Chen Y, Cheng M, et al. The modulatory effect of polyphenols from green tea, oolong tea and black tea on human intestinal microbiota in vitro. Journal of Food Science and Technology. 2018; 55(1): 399-407.
25. Wu Y, Ma N, Song PX, et al. Grape seed proanthocyanidin affects lipid metabolism via changing gut microflora and enhancing propionate prodution in weaned pig. The Journal of Nutrition. 2019; 8: 1523-1532.
26. Fujii K, Ota Y, Nishiyama K, et al. Blueberry leaf polyphenols prevent body fat accumulation in mice fed high-fat, high-sucrose diet. Journal of Oleo Science. 2019; 4: 1-9.
27. Huang, F., Zheng, X., Ma, X. et al. Theabrownin from Pu-erh tea attenuates hypercholesterolemia via modulation of gut microbiota and bile acid metabolism. Nature Communications. 2019; 10(1). Available:https://doi.org/10.1038/s41467-019-12896-x.
28. Velagapudi VR, Hezaveh R, Reigstad CS, et al. The gut microbiota modulates host energy and lipid metabolism in mice. Journal of Lipid Research. 2010; 51: 1101-1112.